Adaptive supertwisting sliding mode control of fuel cell, supercapacitor and battery based plugin hybrid electric vehicle

By

Syed Hayatullah

00000319592

Supervisor

Dr. Iftikhar Ahmad Rana

Department of Electrical Engineering

A thesis submitted in partial fulfillment of the requirements for the degree of

Masters of Science in Electrical Engineering (MS EE)

In

School of Electrical Engineering and Computer Science,

National University of Sciences and Technology (NUST),

Islamabad, Pakistan.

(November 2021)

Approval

It is certified that the contents and form of the thesis entitled "Adaptive Supertwisting Sliding Mode Control of Fuel Cell, Supercapacitor, and Battery based Plugin Hybrid Electric Vehicle" submitted by SYED HAYATULLAH have been found satisfactory for the requirement of the degree

Advisor : Dr. Iftikhar Ahmad Rana

Signature: ______________________

Date: 03-Nov-2021

Committee Member 1:Dr. Safdar Abbas Khan

Signature:

03-Nov-2021

Committee Member 2:Dr. Kamran Zeb

Signature: ______________________

Date: 03-Nov-2021

Signature: ______________________

Date: ______________________

THESIS ACCEPTANCE CERTIFICATE

Certified that final copy of MS/MPhil thesis entitled "Adaptive Supertwisting Sliding Mode Control of Fuel Cell, Supercapacitor, and Battery based Plugin Hybrid Electric Vehicle" written by SYED HAYATULLAH, (Registration No 00000319592), of SEECS has been vetted by the undersigned, found complete in all respects as per NUST Statutes/Regulations, is free of plagiarism, errors and mistakes and is accepted as partial fulfillment for award of MS/M Phil degree. It is further certified that necessary amendments as pointed out by GEC members of the scholar have also been incorporated in the said thesis.

Signature: ____________________

Name of Advisor: Dr. Iftikhar Ahmad Rana

Date: 03-Nov-2021

Signature (HOD): ____________________

Date: ____________________

Signature (Dean/Principal): ____________________

Date: ____________________

Dedication

Dedicated to Respected Teachers specially my supervisor and My family

For their Love, Kindness, and Encouragement

Certificate of Originality

I hereby declare that this submission titled "Adaptive Supertwisting Sliding Mode Control of Fuel Cell, Supercapacitor, and Battery based Plugin Hybrid Electric Vehicle" is my own work. To the best of my knowledge it contains no materials previously published or written by another person, nor material which to a substantial extent has been accepted for the award of any degree or diploma at NUST SEECS or at any other educational institute, except where due acknowledgement has been made in the thesis. Any contribution made to the research by others, with whom I have worked at NUST SEECS or elsewhere, is explicitly acknowledged in the thesis. I also declare that the intellectual content of this thesis is the product of my own work, except for the assistance from others in the project's design and conception or in style, presentation and linguistics, which has been acknowledged. I also verified the originality of contents through plagiarism software.

Student Name:SYED HAYATULLAH

Student Signature: _______________

Acknowledgment

First of all, I would like to express my gratitude to Allah Almighty (SWT) for his abundant blessings. After that, I am sincerely grateful to my supervisor Dr. Iftikhar Ahmad Rana for his priceless guidance, encouragements, devotion, and patience. Without his guidance and positive feedback, this thesis manuscript would not have seen the light of day.

I would like to thanks my guidance and evaluation committee members including Dr. Safdar Abbas Khan and Dr. Kamran Zeb for their precious time, valuable suggestions, and invaluable constructive criticism. I would also like to thanks all my friends and colleagues for their suggestions, encouragement, and continuous support.

Last but not least, I would like to say a big thanks to my family for their endless love, kindness, and encouragement. Without their prayers and continuous support, it would not have been possible to accomplish this milestone.

Table of Contents

List of Figures

List of Tables

Abstract

Nowadays, the world's biggest concern is environmental pollution, decrease of fossil fuel reserves, and the depletion of conventional energy resources. Internal combustion engine (ICE) vehicles use conventional fossil fuels and are one of the major contributors of environmental pollution. Hybrid electric vehicles (HEVs) can play a vital role to cater for these issues because they use renewable energy resources that doesn't pollute the atmosphere. Plug-in hybrid electric vehicles (PHEV) have attracted vehicle manufacturers and consumers because of their ability to charge battery bank using an external charger. This study proposes a hybrid energy storage system (HESS) for PHEV that utilizes fuel cell (FC) as a primary source, with battery and supercapacitor as auxiliary sources. Primary source is connected to a DC-DC boost converter whereas both the secondary sources are connected to DC-DC buck-boost converters. All the sources are connected to a DC bus via these DC converters. In addition, the DC bus is coupled with DC-AC inverter followed by a motor to drive the PHEV. Initially, a mathematical model of DC-DC converter is derived. Nonlinear adaptive supertwisting sliding mode controller (AST-SMC) is then designed for the HESS of PHEV. The external charger contains an AC source and a full-bridge rectifier, followed by a DC-DC buck converter to charge the battery. Adaptive parameter update laws are also designed such that the AST-SMC controller keeps updating itself with time-varying parameters to retain its good performance for a long time. Simulation of the system is performed using MATLAB/Simulink and results are compared with state of the art controllers. Hardware in loop (HIL) testing is used for experimental validation of the system. The results show that the proposed HESS with AST-SMC controller performs well and remains stable under all load requirements of extra urban drive cycle (EUDC).

Chapter 1

Introduction

1.1 Background and Motivation

Renewable energy resources are the best alternative to get clean, cost-effective and perpetual energy. For this, it is important to effectively utilize multiple energy sources [1]. ICE vehicles use conventional fuels. Issue with these fossil fuel vehicles is harmful emissions, declining fossil fuel reserves, and high running cost. HEVs can play a vital role in solving all these problems [2].

Electric vehicles (EVs) have multiple types such as HEVs, battery electric vehicles (BEVs), FC hybrid electric vehicles (FHEVs) and PHEVs. Proton-exchange membrane (PEM) FC is considered a good alternative as it has high efficiency, low temperature, high energy density and zero tailpipe emissions [3], [4] and [5]. HEVs require long driving range and high-power performance but due to chemical reaction of hydrogen with oxygen, PEM FC manifests slow transient and slow startup characteristics. In rapid acceleration and high load conditions, the FC gives limited power response [6], [7]. To cater for the limited power response, PEM FC is integrated with a battery. FC and battery are high power density sources [8]- [9]. Combination of multiple energy resources is known as HESS. Effectively utilizing these resources' balances power and energy density [6]- [10].

FC and battery hybridization is inexpensive, compact, and reliable. By integrating supercapacitor to HESS, PEM FC based HEV gets the ability to cater for high dynamical response and increase the lifetime of power sources [11] and [12]. In general, FC is used as a primary source in the HEV which provides constant load power demand. Excess energy produced by FC and regenerative braking is stored in the energy storage devices. Battery and supercapacitor are used to provide high power demand and high dynamic response. However, to avoid overcharging and discharging, the batteries operate in limited state of charge (*SoC*) range. Supercapacitor is low energy density source and has less backup time [10].

To increase the lifetime of batteries and avoid limited operation, PHEVs have an advanced feature to charge the batteries using electric grid stations which also helps vehicles to take long drive trip and cover long distances [13]. PHEVs consist of AC-DC boost converter followed by bridge rectifier and a DC-DC buck converter connected to the battery terminals [13].

1.2 Problem statement

Various control methods and strategies have been applied to the HESS of PHEVs. The dynamical model of the PHEVs based HESS is developed by [14]. The energy management system consisting of power sources and power converter has a nonlinear behavior; therefore nonlinear control is proposed [14]. Various controllers are applied on the battery and supercapacitor based PHEVs [15]- [16].

FC, battery and supercapacitor-based PHEVs are also proposed in the literature, and few nonlinear controllers are applied but have steady state error, more settling time and chattering phenomenon [17]. Most of the designs use constant values of parameters (i.e., resistors, capacitors, and inductors). The values of these parameters are prone to change with time because of wear and tear, production faults and disturbances [18].

1.3 Proposed approach

In this research, a nonlinear AST-SMC controller is designed for controlling the HESS of FC, battery and supercapacitor-based PHEV and G2V charger. Simulation of this work is done using MATLAB/Simulink software. AST-SMC is robust to parametric variations and external disturbances because the adaptive controller keeps updating itself according to changes in parametric values [18]. The presence of a higher-order derivative in the controller ensures rapid convergence to the sliding manifold in a finite time and goes to the reference point (zero) asymptotically. The proposed AST-SMC algorithm for HESS of PHEVs has faster convergence, less steady-state error and less rise time [17]. Finally, HIL has been done using Delfino C2000 microcontroller (MCU) for checking the real-time validation of the proposed controller. Fig. 1.1 shows the general architecture of the proposed PHEV. The control strategy of the PHEV is divided into two major levels.

1.3.1 Low-level control

This level includes the control of power DC-DC converters, DC to AC inverter, the flow of current in both directions, DC bus voltage and G2V charger voltage

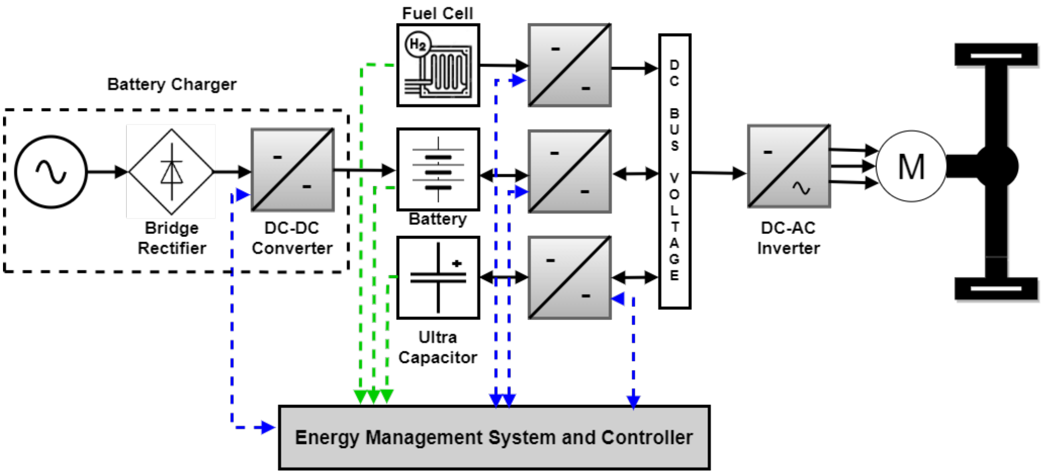

Figure 1.1: Plugin hybrid electric vehicle block diagram

regulation.

1.3.2 High-level control

This control level is for the overall system operation, which ensures the stability of the whole system while monitoring the SoC.

1.4 Contribution

The contribution of the research work is to design a nonlinear controller for the PHEV containing FC, battery and SC sources and G2V charger, which enhance the stability of the system. Adaptation of the unknown parameters of the HESS. the adaptation of the unknown parameters makes the controller more robust against the disturbances. Furthermore, DC bus voltage regulation of the PHEV and cater the chattering phenomena associated with the SMC. To the best of our knowledge, this work has not been discussed in the literature. The key features of this work have the following contributions:

1. Adaptive, robust and fast AST-SMC based nonlinear controller is utilized for energy management of PHEV.

2. Adaptive grid to vehicle charging system is proposed such that the charger keeps working efficiently even if there are parametric variations and uncertainties.

3. DC link voltage regulation and current tracking is achieved in the presence of load variations of EUDC.

4. Adaptive update laws are derived for PHEVs to keep updating the controller to cater for the parametric variations and uncertainties.

5. The designed HESS controller is able to update its parameters by monitoring the wear and tear ensuring good performance for a long time duration.

1.5 Thesis layout

This thesis is arranged as follows: in chapter 2, a literature review in the domain of hybrid electric vehicles has been done. In which different linear and nonlinear control strategies are elaborated in detail. Chapter 3 describes the mathematical modeling of the G2V charger, HESS, and state-space model of the PHEV. Chapter 4 presents the Methodology of the proposed PHEV model. In this energy management algorithm and proposed nonlinear control is designed. Chapter 5 explains simulation as well as experiential results with detailed discussions. Finally, chapter 6 presents the conclusion and future work which can be done.

Chapter 2

Literature Review

2.1 Classification of HEVs

For over one century, traditional ICE have existed. ICE vehicles companies have increased their production due to rise in personal cars usage and this increased issues such as these vehicles are not environmental friendly and they produces green house gases and the depletion of fossil fuels. Transformation companies, government bodies and researches are stimulated to find the aforementioned issues. They proposed the HEV, these vehicles are fuel elective and uses renewable sources. These sources are economical and are pollution free. EVs are categorized into three major types as follow:

1. Hybrid electric vehicles

2. Battery electric vehicles

3. PLug-in hybrid electric vehicles

2.1.1 Hybrid electric vehicles

HEV combines battery powered electric and ICE and sometimes it consist of fuel cell, battery and supercapacitor as sources to track the motor [19]. Battery and supercapacitor are being charged by the ICE or fuel cell during low load driving condition and regenerative breaking of vehicles. SC store energy while the vehicle is deceleration. Fuel efficiency is increased by 25% by using battery in HEV compared to ICE vehicles.

2.1.2 Battery electric vehicles

Battery electric vehicles (BEVs) have no internal combustion motor, it is pure electric vehicles which uses only battery as a source to track the motor, therefore it is also called pure battery vehicles [20]. Battery vehicle needs to be charged after covering limited driving range and then it must be charged using charger connect to gird. Since these vehicles are purely electric and accommodates the driving range of 80 to 100 miles. Battery electric vehicles are environmental friendly vehicles they do not produces harmful emissions and green house gases. However, some grid stations are not based on renewable energy resources therefore, they use fossil fuels to produce the electricity and charges the batteries and produces green house gases. BEVs requirs large battery size and capacity (e.g., 25 to 35kWh).

2.1.3 Plug-in hybrid electric vehicles

Both PHEV and HEV have almost same features and sources. The sources of PHEV can be FC, Battery and SC. FC is used as main source in PHEV and battery and SC are used as energy storage source and used as auxiliary sources.

These sources are connected to power control units [13]. PHEV has external G2V charger to charge the batteries, when they are discharged. Due to inclusion of G2V charger into the HEVs the lifespan of batteries are increased. Since FC is used as main source to drive the motor of PHEV, so the vehicles can be driven to long distance range compare to BEV [21].

2.2 Control technique review

Various control techniques are applied on PHEV including linear and nonlinear control techniques. All these control techniques are used to regulate the DC bus voltage at 400 volt and ensures the stability of the systems [11]. Commonly used linear and nonlinear controller are presented here.

2.2.1 PI/PID controller

Linear controller has been used in almost every controlling plant because this controller is easy to understand and simple to implement. The controller gain tuning makes it robust which provides optimum operation [22]. PI and PID combination is used in different system according to the requirement of system [23]. However, these linear controller can not handle nonlinearities and becomes outdated with the passage of time and gives slow response.

2.2.2 Lyapunov redesign controller

This is basic nonlinear control technique, which track the sources currents and DC bus voltage to their reference points. Design and implementation of lyapunov redesign is easy but it has high steady state error and settling time. Asymptotic stability of the system can not be achieved. [24]

2.2.3 Synergetic controller

This nonlinear controller resembles the sliding mode control because synergetic controller uses macro-variables as sliding surface. These macro-variables incorporates tracking errors which can be one or more depending upon the state model of the system. Asymptotic stability of the system can be ensured by designing the stable macro-variables. This nonlinear control technique gives better results than SMC with no chattering phenomena. It has less settling time but has steady state error and difficult to design [25–27].

2.2.4 Backstepping controller

Backstepping (BS) is recursive Lyapnov-based technique which ensures the closed-loop stability of the system model. Feedback control law and Lyapunov function selection is systematic. BS can only be implemented to the strict feedback form model, if the model is not in this form then we first change the model into strict feedback form and then apply BS. It does not show robustness to external disturbances and varying load conditions [28].

2.2.5 Sliding mode controller

SMC is one of the well known nonlinear controllers which is robust to external disturbances, parametric variations and it is easy to implement. In this technique essential feature is the selection of sliding manifold of the system model. The control law and sliding surface guides the system state to reach to sliding manifold and remain there. The problem with SMC is it suffers from the steady state error and chattering issue, which make he controller less efficient [2, 29].

2.2.6 Integral and double integral SMC

Integral Sliding mode control (ISMC) and double integral sliding mode control (DISMC) is variant of traditional SMC. In ISMC and DISMC adds integral and double integral terms to the sliding surface of the system model. This integral terms help to decrease the transient as well as steady state error [2].

2.2.7 Terminal Sliding mode controller

Terminal sliding mode control (TSMC) shows robustness against nonlinear uncertainties and perturbations. In TMSC the system states trajectories go to the reference point in a finite time [16]. This control technique reduces the chattering issue and steady state error.

2.2.8 Adaptive Nonlinear Controller

In this technique, unknown parameters used in the nonlinear dynamical systems are adapted by using adaptive control laws. This make the control generic and be used in any atmosphere because it can cater internal as well as external disturbances. This also adapt the parametric variation and then adjust the values of parameters. Adaptive controllers have fast convergence to their reference points [15, 16]. Table **??** shows some recent linear and nonlinear controller papers literature review.

Table 2.1: Linear and nonlinear controllers literature review

Sr. No.	Paper	Year	Journal	Technique	Outcome
1	A Lyapunov-based power management for a fuel cell hybrid power source for electric vehicle	2016	Proceedings of 2015 IEEE International Renewable and Sustainable Energy Conference	Lyapunov	Very basic techniques. Easy to design and implement. Asymptotic stability cannot be achieved.
2	Synergetic Control for HIV Infection System of CD4+T Cells	2016	International Conference on Control, Automation And Systems	Synergetic	In synergetic controller a set of macro variables are designed. This controller provides stability characteristics like global stability, handling all kind of noise and parameters insensitivity for smooth operation. It is not complicated but cannot handle the sudden transients.
3	Backstepping control and energy management of hybrid DC source based electric vehicle	2016	4th International Symposium On Environment Friendly Energies And Applications	Backstepping	FC and battery currents are adequately regulated to their references. But backstepping is not robust and does not give finite time convergence.
4	Sliding Mode Control of Fuel Cell and Supercapacitor Hybrid Energy Storage System	2012	IFAC Proceedings Volumes (IFAC Papers Online)	SMC	Nonlinear dynamical model is used to obtain this controller using the defined sliding surface for fast response, but it has chattering issues.

Sr. No.	Paper	Year	Journal	Technique	Outcome
5	Power Split of Fuel Cell/Ultracapacitor Hybrid Power System by Backstepping Sliding Mode Control	2012	IEEE	Backstepping SMC	Backstepping sliding model controller is used to enable the nonlinear system to maintain the stable response under varying dynamics while adapting to load variations. It is relatively robust but complicated and does not give finite-time convergence.
6	Robust speed control of hybrid electric vehicle using fractional order fuzzy PD and PI controllers in cascade control loop	2016	Journal of the Franklin Institute	Fuzzy	FOFPD and FOFPI controllers particularly handles the system variations with time and model uncertainties. This is validated to be the robust nonlinear controllers compared to FPI/FPD.
7	Design and implementation of conventional (PID) and modern (Fuzzy logic) controllers for an energy storage system of hybrid electric vehicles	2018	Proceedings of the IEEE National Aerospace Electronics Conference, NAECON	PID and Fuzzy	PID controller is not perfect for the nonlinear control system but it can be acceptable. Designing this controller is less complicated as compare to FLC but FLC gives a fast response for applications like this system. The computational time of FLC is very high.

Sr. No.	Paper	Year	Journal	Technique	Outcome
8	Adaptive power management of hybrid electric vehicle with neural based PID controller	2018	4th IEEE Uttar Pradesh Section International Conference on Electrical, Computer and Electronics	Adaptive neural PID	The tracing of the drive cycles gives less error contribution in the output. Which simply enhances the performance of the vehicle and afterward increases the overall efficiency of the vehicle. Rule-Based logic is more.
9	Model predictive control for hybrid electric vehicles with linear parameter varying model	2018	International Conference on Control, Automation and Systems	MPC	By providing the predicted speed, MPC reduces fuel consumption and improves the fuel economy at high speed. Training of system requires a long time.
10	Output Voltage Regulation of FC-UC Based Hybrid Electric Vehicle Using Integral Backstepping Control	2019	IEEE Access	Lyapunov redesign and Integral Backstepping	This nonlinear controller helps to remove the steady state error which is present in simple/conventional backstepping controller.

Sr. No.	Paper	Year	Journal	Technique	Outcome
11	Design of integral terminal sliding mode controller for the hybrid AC/DC microgrids involving renewables and energy storage systems	2020	Journal of Electrical Power and Energy Systems	ITSMC	The terminal sliding mode can let the errors of reference and actual values approach zero in a limited time. It is robust and shows a fast dynamic response. It reduced chattering which has been observed in the case of conventional SMC.
12	Multistage adaptive nonlinear control of battery ultracapacitor based plugin hybrid electric vehicles	2020	Journal of Energy Storage	Adaptive Terminal SMC	Adaptive terminal SMC controller model parameters are tuned using a genetic algorithm (GA), the controller adapts the unknown parameters of the system giving fast and robust response and good tracking performance.
13	Barrier function-based adaptive sliding mode control	2018	Automatica	Barrier SMC	First-order systems whose disturbance is bounded with an unknown boundary. It ensures the convergence of the output variable and maintains it in a predefined neighborhood of zero independent of the upper bound of the disturbance, without overestimating the control gain.

Chapter 3

Mathematical Modeling

3.1 Hybrid Energy Storage System Modelling

In this chapter, we present mathematical model of the proposed HESS comprising of a PEM FC, supercapacitor, battery and grid to vehicle (G2V) charger.

3.1.1 Grid to vehicle charger modeling

PHEVs need an external charger to quickly charge the vehicle battery. Multiple types of chargers are proposed in the literature [30]. An external G2V charger reduces weight and cost of PHEV because an external charger is present at a shared charging station.

Mathematical modeling and MATLAB simulations are used to demonstrate the charging performance of G2V PHEV chargers. Rapidly increasing PHEVs and G2V charging stations can result in power factor (PF) adjustment issues and harmonic oscillations [31]. Conventional chargers are unidirectional and use constant voltage (CV) and constant current (CC) charging methods [32]. As compared to bidirectional chargers, unidirectional G2V chargers are more popular because of their safety ratings [33].

The proposed storage system consists of ten batteries of 24 volts each. All batteries are connected in parallel to make a battery pack of 240 volts. Charging time and battery lifespan are important characteristics for measuring G2V charger performance. Charger design depends on the components used and control algorithm applied for efficient charging. The control algorithm ensures smooth charging and rapid transient response [34].

The proposed system is similar to [35] in which a buck converter is used to charge the battery when vehicle is parked at the charging station. Fig. 3.1 shows full bridge rectifier for converting AC-DC followed by resistor-capacitor (RC) filter and a buck converter [36]- [37]. Single-stage AC-DC conversion results in multiple low-frequency ripples in the DC current. Whereas, two-stage power converter for converting AC-DC and then DC-DC results in a small ripple. Therefore, two stage scheme is used to charge batteries having high power rating [38]. *SoC* function shows the level of charge of the battery relative to its capacity:

$$SoC = \frac{C}{C_{nom}} \tag{3.1}$$

where C is real capacity (Ah) and C_{nom} is nominal stored capacity (Ah) of the battery.

SoC and impedance govern the charging voltage of battery V_{ch}. Charging current I_{ch} is governed by energy management algorithm that monitors voltage, *SoC* and temperature of the battery [39]. Following equations show active and reactive power of the grid when it is connected to G2V charger for charging the battery:

$$P = VIcos\theta \tag{3.2}$$

$$Q = VIsin\theta \tag{3.3}$$

where P denotes the active power, Q denotes the reactive power, θ denotes phase angle, V denotes grid voltage and I is the grid current.

Charging power P can be represented in terms of charging source efficiency η as:

$$P = \eta VI\cos\theta \tag{3.4}$$

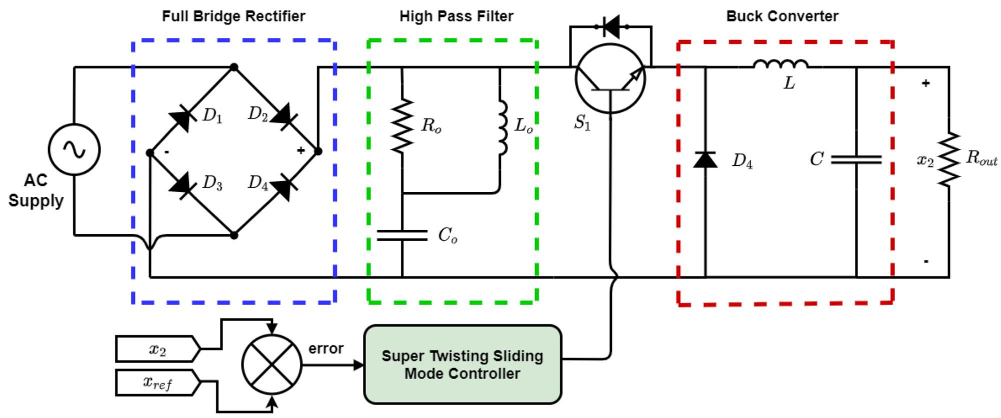

Figure 3.1: PHEV G2V charger model

The DC-DC buck converter consists of a diode D, inductor L, capacitor C, resistance R and a switch S. Inductor volt second and capacitor charge balance equations are used to derive the state space model of the buck converter used in V2G charger given as:

$$\left.\begin{aligned} \dot{x}_1 &= -\frac{x_2}{L} + \frac{V_g\mu}{L} \\ \dot{x}_2 &= -\frac{V_g\mu}{RC} + \frac{x_1}{C} \end{aligned}\right\} \tag{3.5}$$

where x_1 is the average inductor current $< I_{L1} >$, x_2 is the average output voltage $< V_{ch} >$ and μ is the control input.

The parameters L, C and RC used in eq. (3.5) are difficult to calculate. These parameters vary slowly with time and for using them in the design procedure of the adaptive controller, we make following replacements:

$$\theta_1 = \frac{1}{L}; \quad \theta_2 = \frac{1}{C}; \quad \theta_3 = \frac{1}{RC} \tag{3.6}$$

where θ_1, θ_2 and θ_3 are time-varying parameters. Substituting the time-varying parameters from eq. (3.6) to HESS model eq. (3.5), the G2V charger modeling can be presented as:

$$\left.\begin{aligned} \dot{x}_1 &= \theta_1 V_g\mu - \theta_1 x_2 \\ \dot{x}_2 &= \theta_2 x_1 - \theta_3 V_g\mu \end{aligned}\right\} \tag{3.7}$$

In model (3.7), the G2V charger model is obviously MIMO nonlinear system, so a nonlinear controller is required.

3.1.2 Hybrid energy storage system modeling:

In this section, the mathematical model of HESS is presented. Fig. 3.2 shows the model of HESS for the PHEV. This includes DC-DC converters when connected to FC, battery and supercapacitor. The proposed system consists of inductors L_1, L_2, L_3 with resistors R_1, R_2, R_3, a diode D_1, capacitor C_0 and switches S_1, S_2, S_3, S_4, S_5 of IGBT controlled by the input gate signals u_1, u_{23}, and u_{45}.

FC operation

FC is connected to DC-DC boost converter that connects the FC to DC bus. It consists of switch S_1, with two states, which decides operating modes of the converter [15]. Following mathematical model of the boost converter can be obtained by applying Kirchhoff Voltage law:

$$\frac{di_{fc}}{dt} = \frac{1}{L_1}[V_{fc} - R_1 i_{fc} - (1-u_1)V_0] \tag{3.8}$$

$$\frac{dV_0}{dt} = \frac{1}{C_0}[i_{fc}(1-u_1) - i_1] \tag{3.9}$$

where i_{fc} represents input current of the inductor, i_1 represents output current of the converter, V_{fc} represents the voltage of FC, u_1 represents the control input and V_0 represents the output voltage of converter.

Battery operation

Battery is connected to DC-DC buck-boost converter that connects the battery to DC bus. It consists of switches S_2 and S_3 [15].

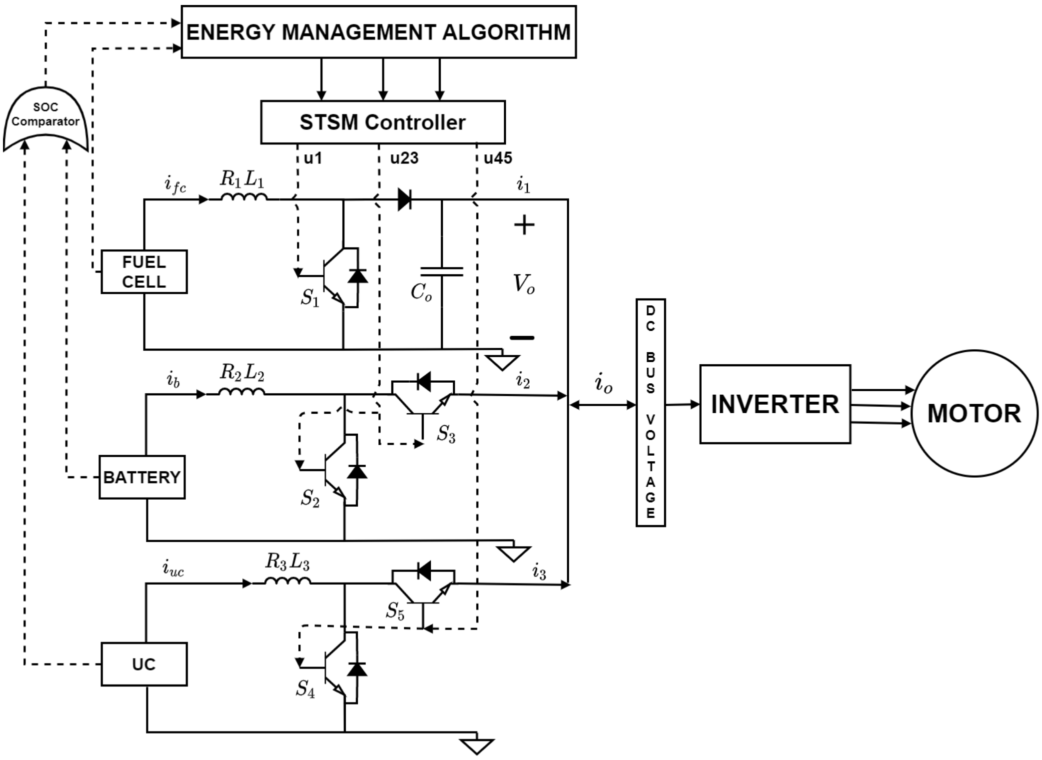

Figure 3.2: Circuit diagram of HESS of PHEV

When S_3 is OFF $(i_b > 0)$ and S_2 is ON, the converter works as a boost converter in discharging mode. When S_3 is ON $(i_b < 0)$ and S_2 is OFF, the converter works as a buck converter in charging mode. During discharging, the mathematical model of the converter is expressed as:

$$\frac{di_b}{dt} = \frac{1}{L_2}[-R_2 i_b + V_b - (1-u_2)V_o] \tag{3.10}$$

where u_2 is control input, battery current is represented by i_b and battery voltage is represented by V_b. During charging, the mathematical model of the converter can be expressed as:

$$\frac{di_b}{dt} = \frac{1}{L_2}[-R_2 i_b + V_b - u_3 V_o] \tag{3.11}$$

where u_3 is control input, i_2 is the output current from buck-boost converter. For the combine equation of buck-boost converter in terms of variable G is defined as:

$$G = \begin{cases} 1, \ if \ i_{bref} > 0 \quad (Boost) \\ 0, \ if \ i_{bref} < 0 \quad (Buck) \end{cases}$$

where i_{bref} is the reference current of the battery. Combined mathematical model of battery converter can be obtained as:

$$u_{23} = G(1 - u_2) + (1 - G)u_3 \tag{3.12}$$

Hence, the global battery model can be written as:

$$\frac{di_b}{dt} = \frac{1}{L_2}[-R_2 i_b + V_b - u_{23} V_o] \tag{3.13}$$

The output current equation will be written as:

$$i_2 = u_{23} i_b \tag{3.14}$$

Supercapacitor operation

Supercapacitor is connected to DC-DC buck-boost converter that connects the battery to the DC bus. Since the battery UC current flows in both directions so it has both charging and discharging properties. Combined equations for charging and discharging can be obtained in the same manner. Defining variable G as:

$$G = \begin{cases} 1,\ if\ i_{scref} > 0 \quad (Boost) \\ 0,\ if\ i_{scref} < 0 \quad (Buck) \end{cases}$$

where i_{ucref} is the reference current of the supercapacitor. Combined mathematical model of battery converter can be obtained as:

$$u_{45} = G(1-u_4) + (1-G)u_5 \tag{3.15}$$

Hence, the global model of the battery is written as:

$$\frac{di_{sc}}{dt} = \frac{1}{L_3}[-R_3 i_{sc} + V_{sc} - u_{45}V_0] \tag{3.16}$$

The output current equation will be written as:

$$i_3 = u_{45} i_{sc} \tag{3.17}$$

HESS global modelling

From fig. 3.2 one can find the output current (i_o) equation using Kirchhoff current law (KCL).

$$i_0 = i_1 + i_2 + i_3. \tag{3.18}$$

Substituting values of i_2 and i_3 from eq. (3.14) and eq. (3.17) in eq. (3.18):

$$i_1 = i_0 - u_{23} i_b - u_{45} i_{sc} \tag{3.19}$$

Substituting the value of i_1 from eq. (3.9) in eq. (3.19) gives:

$$\frac{dV_0}{dt} = \frac{1}{C_0}[(1-u_1)i_{fc} + u_{23} i_b + u_{45} i_{sc} - i_0] \tag{3.20}$$

State space model

For controller design, the average control model is used by averaging it for one time period and replacing $< i_{fc} >$, $< i_b >$, $< i_{uc} >$ and $< V_o >$ by x_1, x_2, x_3 and x_4 respectively, we get:

$$\left.\begin{aligned}
\dot{x}_1 &= -\frac{R_1}{L_1}x_1 + \frac{1}{L_1}V_{fc} - \frac{1-u_1}{L_1}x_4 \\
\dot{x}_2 &= -\frac{R_2}{L_2}x_2 + \frac{1}{L_2}V_b - \frac{u_{23}}{L_2}x_4 \\
\dot{x}_3 &= -\frac{R_3}{L_3}x_3 + \frac{1}{L_3}V_{sc} - \frac{u_{45}}{L_3}x_4 \\
\dot{x}_4 &= \frac{1}{C_0}[(1-u_1)x_1 + u_{23}x_2 + u_{45}x_3 - i_0]
\end{aligned}\right\} \tag{3.21}$$

The parameters R_1, R_2, R_3, L_1, L_2, L_3 and C used in eq. (3.21) are difficult to get precisely in practice. Considering these parameters as time-varying and incorporating them in the design procedure of the adaptive controller, the unknown parameters in the HESS model can be defined as follows:

$$\left.\begin{aligned} \theta_1 &= \frac{1}{L_1} = \frac{1}{L_2} = \frac{1}{L_3} \\ \theta_2 &= \frac{R_1}{L_1} = \frac{R_2}{L_2} = \frac{R_3}{L_3} \\ \theta_3 &= \frac{1}{C_0} \end{aligned}\right\} \tag{3.22}$$

Substituting the time-varying parameters from eq. (3.22) in eq. (3.21), the HESS modeling can be simplified as:

$$\left.\begin{aligned} \dot{x}_1 =& -\theta_2 x_1 - (1-u_1)\theta_1 x_4 + \theta_1 x_1 \\ \dot{x}_2 =& -\theta_2 x_2 - u_{23}\theta_1 x_4 + \theta_1 x_2 \\ \dot{x}_3 =& -\theta_2 x_3 - u_{45}\theta_1 x_4 + \theta_1 x_3 \\ \dot{x}_4 =& \theta_3[(1-u_1)x_1 + u_{23}x_2 + u_{45}x_3 - i_O] \end{aligned}\right\} \tag{3.23}$$

The eq. (3.23) shows that HESS is MIMO nonlinear system, so it is necessary to design an effective nonlinear control strategy.

Chapter 4

Methodology

4.1 Energy Management Algorithm for Plugin Hybrid Electric Vehicle

Fig. 4.1 shows the energy management algorithm of the PHEV for an efficient management of energy sources. The proposed energy management algorithm is designed by keeping in view following requirements:

- Efficient distribution of power according to load requirements.
- Equal utilization of all power sources such that none of them is over-loaded.
- Smart management of power such that the *SoC* of the battery and the super-capacitor stay within safe limits for extended operation.

Keeping in view the *SoC* of power sources and load variations, following two modes of operation are defined:

1. During parking mode ($SoC \leq 15\%$), the vehicle battery will be charged

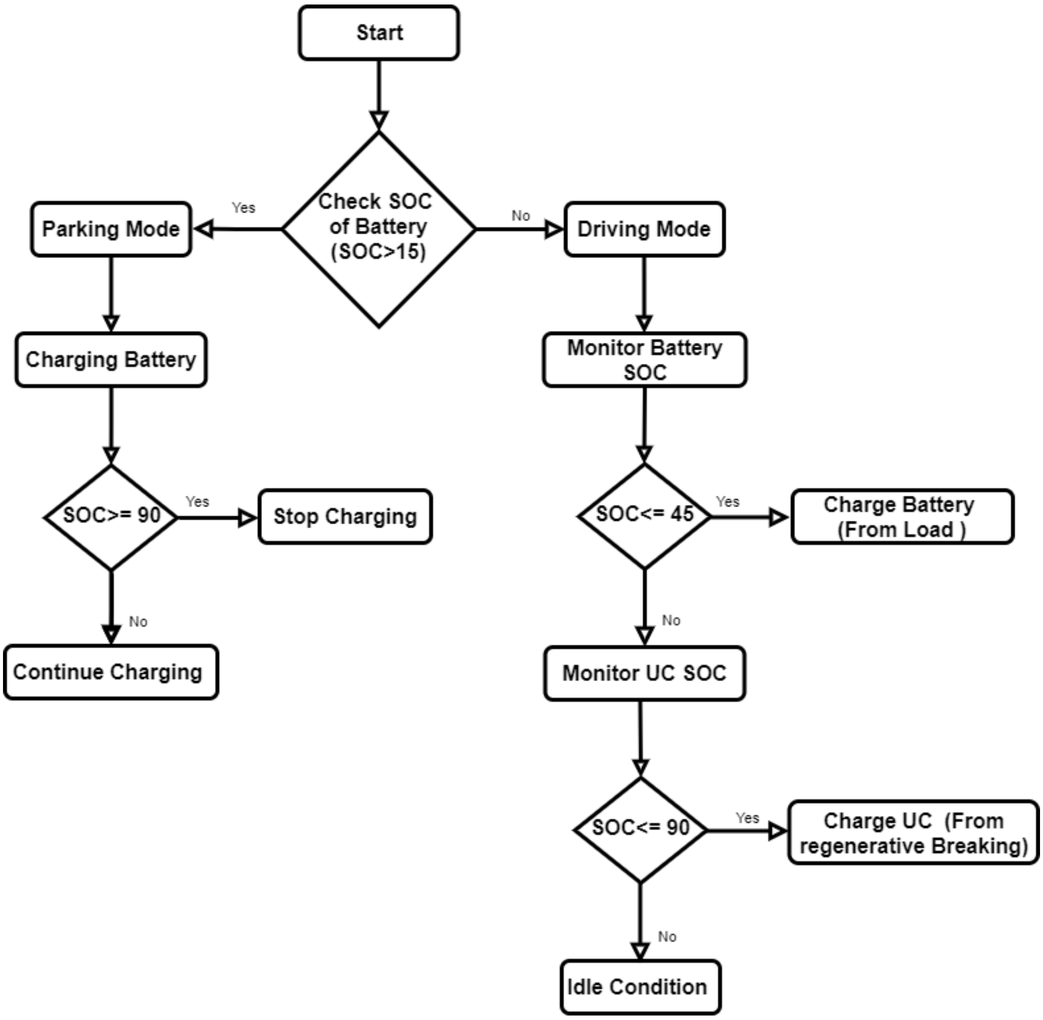

Figure 4.1: Flow chart of battery and supercapacitor state of charge

using proposed G2V charger until the battery is charged to 90% of its maximum capacity. When the battery reaches 90%, the charging will be stopped.

2. During driving mode (*SoC* $\geq$ 15%), the *SoC* of vehicle battery will be continuously monitored. FC and battery will supply the required load. Here battery will be used for the normal load and the supercapacitor for the transient load conditions. If the *SoC* of the battery is less than 45%, then battery will be charged from the load. If the battery *SoC* is more than or equal to 45%, controller will

monitor the *SoC* of supercapacitor. If supercapacitor *SoC* is less than 90%, the supercapacitor will be charged using excess energy from FC, battery and regenerative braking. The *SoC* of the battery and the UC are represented by following equations:

$$SoC_b = SoC_{b_i} - \frac{1}{3600C_b}\int i_b dt \tag{4.1}$$

$$SoC_{sc} = SoC_{sc_i} - \frac{1}{3600C_{sc}}\int i_{sc} dt \tag{4.2}$$

where SoC_b is the present state of charge of the battery, SoC_{sc} is the present state of charge of the SC, SoC_{b_i} is initial state of charge of battery, SoC_{sc_i} is the initial state of charge of the supercapacitor; C_b and C_{sc} are the capacities of battery and supercapacitor respectively.

4.2 Controller Design and stability analysis

To achieve the control objectives, AST-SMC based controller is designed for charger system and energy management system of the PHEV.

4.2.1 Controller design of charger

For ensuring the DC bus regulation of PHEV, the DC-DC buck converter is used to provide fast charging and increased safety. For designing AST-SMC based charger, following current and voltage errors are defined to track the values to the desired reference points:

$$\left.\begin{aligned} e_1 &= x_1 - x_{1ref} \\ e_2 &= x_2 - x_{2ref} \end{aligned}\right\} \tag{4.3}$$

where x_{1ref}=I_{Lref} and x_{2ref}=V_{ref}. I_{Lref} and V_{ref} are the references of inductor current and output voltage respectively. Due to non-minimum phase behaviour of buck converter, x_2 state tracks the reference value directly. Taking time derivative of eq. (4.3), and substituting the value of $\dot{x}_2$ from eq. (3.7), we get:

$$\dot{e}_2 = \dot{x}_2 - \dot{x}_{2ref} = \theta_2 x_1 - \theta_3 V_g \mu - \dot{x}_{2ref} \tag{4.4}$$

Defining the following sliding surface of AST-SMC to get the control law μ of the charger:

$$s_2 = c_2 e_2 \tag{4.5}$$

where c_2 is gain parameter of the sliding surface of AST-SMC having positive constant value. Taking time derivative of the sliding surface eq. (4.5), we get:

$$\dot{s}_2 = c_2 \dot{e}_2 \tag{4.6}$$

Substituting the value of $\dot{e_2}$ from eq. (4.4) in eq. (4.6) yields:

$$\dot{s}_2 = c_2[\theta_2 x_1 - \theta_3 V_g \mu - \dot{x}_{2ref}] \tag{4.7}$$

To ensure the finite time convergence of the AST-SMC controller, the corresponding adaptive estimation errors $\tilde{\theta}_1$, $\tilde{\theta}_2$ and $\tilde{\theta}_3$ are defined for θ_1, θ_2 and θ_3 respectively as:

$$\left.\begin{aligned}\tilde{\theta}_1 = \hat{\theta}_1 - \theta_1\\ \tilde{\theta}_2 = \hat{\theta}_2 - \theta_2\\ \tilde{\theta}_3 = \hat{\theta}_3 - \theta_3\end{aligned}\right\} \tag{4.8}$$

Consider Lyapunov candidate function (LCF) is defined for the asymptotic stability of the controller given as:

$$V = \frac{1}{2}s_2^2 + \frac{1}{2\gamma_1}\,\tilde{\theta}_2^2 + \frac{1}{2\gamma_2}\,\tilde{\theta}_3^2 \tag{4.9}$$

where γ_2 and γ_3 are the gain parameters of adaptive law. Taking time derivative of eq. (4.9), we get:

$$\dot{V} = s_2\dot{s}_2 + \frac{1}{\gamma_1}\,\tilde{\theta}_2\,\dot{\hat{\theta}}_2 + \frac{1}{\gamma_2}\,\tilde{\theta}_3\,\dot{\hat{\theta}}_3 \tag{4.10}$$

Substituting the value of $\dot{s}_2$ from eq. (4.7) into eq. (4.10):

$$\dot{V} = s_2c_2[\theta_2x_1 - \theta_3V_g\mu - \dot{x}_{2ref}] + \frac{1}{\gamma_1}\,\tilde{\theta}_2\,\dot{\hat{\theta}}_2 + \frac{1}{\gamma_2}\,\tilde{\theta}_3\,\dot{\hat{\theta}}_3 \tag{4.11}$$

To obtain the adaptive control incorporated with AST-SMC, eq. (4.11) becomes:

$$\dot{V} = s_2c_2(\hat{\theta}_2 x_1 - \hat{\theta}_3 V_g \mu - \dot{x}_{2ref}) + \tilde{\theta}_2(\frac{1}{\gamma_1}\dot{\hat{\theta}}_2 - s_2c_2x_1) + \tilde{\theta}_3(\frac{1}{\gamma_2}\dot{\hat{\theta}}_3 + s_2c_2v_g\mu) \tag{4.12}$$

Keeping in view the boundedness of time-varying parameters, following adaptive parameter update laws are defined:

$$\dot{\hat{\theta}}_2 = \gamma_1 proj(\hat{\theta}_2, s_2c_2x_1) \tag{4.13}$$

$$\dot{\hat{\theta}}_3 = -\gamma_2 proj(\hat{\theta}_2, s_2c_2v_g\mu) \tag{4.14}$$

Note that a priori information about boundedness of uncertain slowly-varying parameters is required in sliding mode control. Keeping in view the boundedness of slowly varying parameters, following $\mathrm{Proj}_{\hat{\theta}}$ operator is defined:

$$\mathrm{Proj}_{\hat{\theta}} = \begin{cases} 0 & \text{if } \hat{\theta} = \hat{\theta}_{\max} \text{ and } \tau > 0 \\ 0 & \text{if } \hat{\theta} = \hat{\theta}_{\max} \text{ and } \tau < 0 \\ \tau & \text{otherwise} \end{cases}$$

where $\hat{\theta}_{\max}$ is the upper bound of $\hat{\theta}$. $\mathrm{Proj}_{\hat{\theta}}$ stands for projection operator which guarantees boundedness of the estimated parameters by projecting them to bound intervals [40]- [41]. For the asymptotic stability of charging source using AST-SMC controller, taking $\dot{s}_2$ that meets the stability constraint requirements and equating it with eq. (4.7), gives:

$$
\begin{aligned}
\dot{s}_2 &= a_1|s_1|^{\beta} sgn(\frac{s_1}{\phi_1}) - a_2 \int sgn(\frac{s_1}{\phi_1})dt \\
&= c_2[\hat{\theta}_2 x_1 - \hat{\theta}_3 V_g \mu - \dot{x}_{2ref}]
\end{aligned}
\tag{4.15}
$$

Note that $|s_1|^{\beta}$ ensures the convergence of the system to the sliding manifold and ϕ_1 is used for reducing the chattering effect. a_1 and a_2 are positive gains. *sgn* is signum function defined below:

$$
sgn(x) = \begin{cases} \frac{x}{|x|}, & x \neq 0 \\ 0, & x = 0 \end{cases}
$$

Supertwisting sliding mode algorithm with saturation function for reduced chattering can be introduced as:

$$
\begin{aligned}
\mu_{sw} &= a_1|s_1|^{\beta} sgn(\frac{s_1}{\phi_1}) + \mu \\
\dot{\mu} &= a_2 \int sgn\frac{s_1}{\phi_1}dt
\end{aligned}
$$

Solving eq. (4.15) for μ, we get:

$$
\begin{aligned}
\mu = \frac{1}{\hat{\theta}_3 V_g}[\frac{a_1}{c_2}|s_1|^{\beta} sgn(\frac{s_1}{\phi_1}) + \frac{a_2}{c_2}\int sgn(\frac{s_1}{\phi_1})dt \\
+\hat{\theta}_2 x_1 - \dot{x}_{2ref}]
\end{aligned}
\tag{4.16}
$$

For the stability analysis, substituting the values of $\dot{\hat{\theta}}_2$, $\dot{\hat{\theta}}_3$ and μ into eq. (4.12) gives:

$$
\dot{V} = -s_2 a_1 |s_1| sgn(\frac{s_1}{\phi_1}) - s_2 a_2 \int sgn(\frac{s_1}{\phi_1})dt \leq 0
$$

Lyapunov stability analysis shows that the proposed controller is asymptotic stable.

4.2.2 Control design of energy management system of PHEV

AST-SMC controller is designed for the PHEV to give regulated DC bus voltage and accurate charging voltage for all possible (low speed, high speed, steady and transient) loads. The designed controller should be able to track the source currents and DC bus voltage to the desired values in efficient and effective way. It should also be able to monitor the *SoC* of battery and supercapacitor. Stability is also a requirement in the controller design.

To ensure the DC bus voltage regulation of PHEV, the DC-DC buck converter should cater for parametric variations and model uncertainties. The boost converter shows a non-minimum phase behaviour. Output voltage of the converter is regulated indirectly by regulating the input current. The inductor input current i_{fc} tracks the desired reference current i_{fcref} according to the law of conservation of energy [42]. Output power is represented by the following equation:

$$P_0 = P_{fc} + P_b + P_{sc} \tag{4.17}$$

where P_0 is output power, P_{fc} is fuel cell power, P_b is battery power and P_{sc} is the supercapacitor power. Rearranging output power equation (40), the reference power for FC can be obtained as:

$$P_{fcref} = \lambda \left(P_{0_{ref}} - P_{uc_{ref}} - P_{b_{ref}} \right) \tag{4.18}$$

where λ is identity factor and its value must be greater than 1. Rearranging output power equation (45), the reference current for FC can be obtained as:

$$i_{fcref} = \lambda \left[\frac{(V_0 * i_0) - (V_{uc} * i_{uc}) - (V_b * i_b)}{V_{fc}} \right] \tag{4.19}$$

For designing the AST-SMC, the following current and voltage errors are defined to track the values to the desired reference points:

$$e_i = x_i - x_{iref}, \quad \forall\, i = 1,2,3,4. \tag{4.20}$$

For the regulation of the DC bus voltage of energy management system, the error terms must go to zero. Taking time derivative of eq. (4.20) gives:

$$\left.\begin{aligned} \dot{e}_1 &= \dot{x}_1 - \dot{x}_{ref} \\ \dot{e}_2 &= \dot{x}_2 - \dot{x}_{ref} \\ \dot{e}_3 &= \dot{x}_3 - \dot{x}_{ref} \\ \dot{e}_4 &= \dot{x}_4 - \dot{x}_{ref} \end{aligned}\right\} \tag{4.21}$$

Substituting the values of $\dot{x_1}$, $\dot{x_2}$, $\dot{x_3}$ and $\dot{x_4}$ from eq. (3.23) in eq. (4.21) gives:

$$\left.\begin{aligned} \dot{e}_1 &= -\theta_2 x_1 - (1-u_1)\theta_1 x_4 + \theta_1 x_1 - \dot{x}_{1ref} \\ \dot{e}_2 &= -\theta_2 x_2 - u_{23}\theta_1 x_4 + \theta_1 x_2 - \dot{x}_{2ref} \\ \dot{e}_3 &= -\theta_2 x_3 - u_{45}\theta_1 x_4 + \theta_1 x_3 - \dot{x}_{3ref} \\ \dot{e}_4 &= \theta_3((1-u_1)x_1 + u_{23}x_2 + u_{45}x_3 - i_O - \dot{x}_{4ref}) \end{aligned}\right\} \tag{4.22}$$

Defining the sliding surface of AST-SMC to get the control laws u_1, u_{23} and u_{45}

of PHEV as:

$$s_i = c_i e_i \quad \forall\, i = 1,2,3,4 \tag{4.23}$$

where c_i is gain parameter of the sliding surface of AST-SMC having positive constant value. Taking time derivative of the sliding surface eq. (4.23), we get:

$$\dot{s}_1 = c_1\dot{e}_1;\ \dot{s}_2 = c_2\dot{e}_2;\ \dot{s}_3 = c_3\dot{e}_3;\ \dot{s}_4 = c_3\dot{e}_4 \tag{4.24}$$

Now substituting the values of $\dot{e}_1$, $\dot{e}_2$, $\dot{e}_3$ and $\dot{e}_4$ from eq. (4.22) in eq. (4.24), we get:

$$\left.\begin{aligned}
\dot{s}_1 &= c_1[-\theta_2 x_1 - (1-u_1)\theta_1 x_4 + \theta_1 x_1 - \dot{x}_{1ref}] \\
\dot{s}_2 &= c_2[-\theta_2 x_2 - u_{23}\theta_1 x_4 + \theta_1 x_2 - \dot{x}_{2ref}] \\
\dot{s}_3 &= c_3[-\theta_2 x_3 - u_{45}\theta_1 x_4 + \theta_1 x_3 - \dot{x}_{3ref}] \\
\dot{s}_4 &= c_4[(1-u_1)\theta_3 x_1 + u_{23}\theta_3 x_2 + u_{45}\theta_3 x_3 - \theta_3 i_O \\
&\quad - \dot{x}_{4ref}]
\end{aligned}\right\} \tag{4.25}$$

To ensure the finite time convergence of the AST-SMC controller, the corresponding adaptive estimation errors $\tilde{\theta}_1$, $\tilde{\theta}_2$ and $\tilde{\theta}_3$ are defined for θ_1, θ_2 and θ_3 respectively as:

$$\left.\begin{aligned}
\tilde{\theta}_1 &= \hat{\theta}_1 - \theta_1 \\
\tilde{\theta}_2 &= \hat{\theta}_2 - \theta_2 \\
\tilde{\theta}_3 &= \hat{\theta}_3 - \theta_3
\end{aligned}\right\} \tag{4.26}$$

Following Lyapunov candidate function is defined for the asymptotic stability of the controller:

$$V = \frac{1}{2}(s_1^2 + s_2^2 + s_3^2 + s_4^2 + \frac{1}{\gamma_1}\ \tilde{\theta}_2^2 + \frac{1}{\gamma_2}\ \tilde{\theta}_2^2 + \frac{1}{\gamma_3}\ \tilde{\theta}_3^2) \tag{4.27}$$

where γ_1, γ_2, and γ_3 are the gain parameters of adaptive law. Taking time derivative of eq. (4.27) gives:

$$\begin{aligned} \dot{V} = s_1\dot{s}_1 + s_2\dot{s}_2 + s_3\dot{s}_3 + s_4\dot{s}_4 + \frac{1}{\gamma_1}\ \tilde{\theta}_1\ \dot{\hat{\theta}}_1 \\ + \frac{1}{\gamma_2}\ \tilde{\theta}_2\ \dot{\hat{\theta}}_2 + \frac{1}{\gamma_3}\ \tilde{\theta}_3\ \dot{\hat{\theta}}_3 \end{aligned} \tag{4.28}$$

Substituting the values of $\dot{s}_1$, $\dot{s}_2$, $\dot{s}_3$ and $\dot{s}_4$ from eq. (4.25) in eq. (4.28) yields:

$$\left.\begin{aligned} \dot{V} = s_1c_1[-\theta_2x_1 - (1-u_1)\theta_1x_4 + \theta_1x_1 - \dot{x}_{1ref}] \\ + s_2c_2[-\theta_2x_2 - u_{23}\theta_1x_4 + \theta_1x_2 - \dot{x}_{2ref}] \\ + s_3c_3[-\theta_2x_3 - u_{45}\theta_1x_4 + \theta_1x_3 - \dot{x}_{3ref}] \\ + s_4c_4[(1-u_1)\theta_3x_1 + u_{23}\theta_3x_2 + u_{45}\theta_3x_3 - \theta_3i_O \\ - \dot{x}_{4ref}] + \frac{1}{\gamma_1}\ \tilde{\theta}_1\ \dot{\hat{\theta}}_1 + \frac{1}{\gamma_1}\ \tilde{\theta}_2\ \dot{\hat{\theta}}_2 + \frac{1}{\gamma_2}\ \tilde{\theta}_3\ \dot{\hat{\theta}}_3 \end{aligned}\right\} \tag{4.29}$$

Incorporating the adaptive control estimators from eq. (4.26) in the eq. (4.29):

$$\left.\begin{aligned}\dot{V} = s_1c_1[-\hat{\theta}_2x_1 + \tilde{\theta}_2x_1 - \hat{\theta}_1(1-u_1)x_4\\ + \tilde{\theta}_1(1-u_1)x_4 + \hat{\theta}_1x_1 - \tilde{\theta}_1x_1 - \dot{x}_{1ref}]\\ +s_2c_2[-\hat{\theta}_2x_2 + \tilde{\theta}_2x_2 - \hat{\theta}_1u_{23}x_4 + \tilde{\theta}_1u_{23}x_4\\ +\hat{\theta}_1x_2 - \tilde{\theta}_1x_2 - \dot{x}_{2ref}] + s_3c_3[-\hat{\theta}_2x_3 + \tilde{\theta}_2x_3\\ -\hat{\theta}_1u_{45}x_4 + \tilde{\theta}_1u_{45}x_4 + \hat{\theta}_1x_3 - \tilde{\theta}_1x_3 - \dot{x}_{3ref}]\\ +s_4c_4[(1-u_1)\hat{\theta}_3x_1 - (1-u_1)\tilde{\theta}_3x_1 + u_{23}\hat{\theta}_3x_2\\ -u_{23}\tilde{\theta}_3x_2 + u_{45}\hat{\theta}_3x_3 - u_{45}\tilde{\theta}_3x_3 - \hat{\theta}_3i_o + \tilde{\theta}_3i_o\\ -\dot{x}_{4ref}] + \frac{1}{\gamma_1}\tilde{\theta}_1\dot{\hat{\theta}}_1 + \frac{1}{\gamma_2}\tilde{\theta}_2\dot{\hat{\theta}}_2 + \frac{1}{\gamma_3}\tilde{\theta}_3\dot{\hat{\theta}}_3\end{aligned}\right\} \tag{4.30}$$

Rearranging the $\dot{V}$ in eq. (4.30) gives:

$$\left.\begin{aligned}\dot{V} = s_1c_1[-\hat{\theta}_2x_1 - (1-u_1)\hat{\theta}_1x_4 + \hat{\theta}_1x_1 - \dot{x}_{1ref}]\\ +s_2c_2[-\hat{\theta}_2x_2 - u_{23}\hat{\theta}_1x_4 + \hat{\theta}_1x_2 - \dot{x}_{2ref}] + s_3c_3[-\hat{\theta}_2x_3\\ -u_{45}\hat{\theta}_1x_4 + \hat{\theta}_1x_3 - \dot{x}_{3ref}] + s_4c_4[(1-u_1)\hat{\theta}_3x_1\\ +u_{23}\hat{\theta}_3x_2 + u_{45}\hat{\theta}_3x_3 - \hat{\theta}_3i_o - \dot{x}_{4ref}] + \tilde{\theta}_1(\frac{1}{\gamma_1}\dot{\hat{\theta}}_1\\ +s_1c_1((1-u_1)x_4 + x_1) + s_2c_2u_{23}x_4 - s_2c_2x_2 +\\ s_3c_3(u_{45}x_4 - x_3)) + \tilde{\theta}_2(\frac{1}{\gamma_2}\dot{\hat{\theta}}_1 +\\ s_1c_1x_1 + s_2c_2x_2 + s_2c_2x_2)\\ + \tilde{\theta}_3(\frac{1}{\gamma_3}\dot{\hat{\theta}}_1 - s_4c_4(1-u_1)x_1 - s_4c_4u_{23}x_2\\ -s_4c_4u_{45}x_3 + s_4c_4i_0)\end{aligned}\right\} \tag{4.31}$$

Keeping in view the boundedness of time-varying parameters, following adaptive parameter update laws are defined:

$$\left.\begin{aligned}\dot{\hat{\theta}}_1 = \gamma_1 proj(\hat{\theta}_1, -s_1c_1(1-u_1)x_4 - s_1c_1x_1\\ -s_2c_2u_{23}x_4 + s_2c_2x_2 - s_3c_3u_{45}x_4 + s_3c_3x_3)\\ \dot{\hat{\theta}}_2 = \gamma_2 proj(\hat{\theta}_2, -s_1c_1x_1 - s_2c_2x_2 - s_2c_2x_2)\\ \dot{\hat{\theta}}_3 = \gamma_3 proj(\hat{\theta}_3,\ s_4c_4(1-u_1)x_1 + s_4c_4u_{23}x_2\\ +s_4c_4u_{45}x_3 - s_4c_4i_0)\end{aligned}\right\} \tag{4.32}$$

To ensure asymptotic stability of energy management system of PHEV using AST-SMC controller, we use the $\dot{s_1}$, $\dot{s_2}$, $\dot{s_3}$ and $\dot{s_4}$ in eq. (4.31) and perform following substitutions:

$$\left.\begin{aligned}-a_1|s_1|^{\alpha} sgn(\frac{s_1}{\phi_1}) - a_2\int sgn(\frac{s_1}{\phi_1})dt\\ = c_1[-\hat{\theta}_2x_1 - (1-u_1)\hat{\theta}_1x_4 + \hat{\theta}_1x_1 - \dot{x}_{1ref}],\\ -a_3|s_2|^{\beta} sgn(\frac{s_2}{\phi_2}) - a_4\int sgn(\frac{s_2}{\phi_2})dt\\ = c_2[-\hat{\theta}_2x_2 - u_{23}\hat{\theta}_1x_4 + \hat{\theta}_1x_2 - \dot{x}_{2ref}],\\ -a_5|s_3|^{\gamma} sgn(\frac{s_3}{\phi_3}) - a_6\int sgn(\frac{s_3}{\phi_3})dt\\ = c_3[-\hat{\theta}_2x_3 - u_{45}\hat{\theta}_1x_4 + \hat{\theta}_1x_3 - \dot{x}_{3ref}]\end{aligned}\right\} \tag{4.33}$$

where a_1, a_2, a_3, a_4, a_5, and a_6 are positive gains, $|s_1|^{\alpha}$, $|s_2|^{\beta}$, and $|s_3|^{\gamma}$ ensure the convergence of system to the sliding manifold and are used to minimize the chattering effect.

Table 4.1: Parameters of G2V charger

G2V Voltage	220V
Frequency	50Hz
Resistance R_0, R	20Ω, $15m\Omega$
Capacitance C_0, C	$50\mu F$, $1mF$
Inductance L_0, L	$4.2mH$, $10mH$

Table 4.2: Specification of power sources

PEM Fuel Cell	350V, 20kW
Li-ion Battery	230VDC, 30Ah
Supercapacitor	205VDC, 2700F

Solving eq. (4.33) for u_1, u_{23} and u_{45}, we get:

$$\left.\begin{aligned} u_1 &= 1 - \frac{1}{\hat{\theta}_1 x_4}[\frac{a_1}{c_1}|s_1|^\beta sgn(\frac{s_1}{\phi_1}) + \frac{a_2}{c_1}\int sgn(\frac{s_1}{\phi_1})dt \\ &\qquad -\hat{\theta}_2 x_1 + \hat{\theta}_1 x_1 + \dot{x}_{1ref}] \\ u_{23} &= \frac{1}{\hat{\theta}_2 x4}[\frac{a_3}{c_2}|s_1|^\beta sgn(\frac{s_1}{\phi_1}) + \frac{a_4}{c_2}\int sgn(\frac{s_1}{\phi_1})dt \\ &\qquad -\hat{\theta}_2 x_2 + \hat{\theta}_1 x_2 - \dot{x}_{2ref}] \\ u_{45} &= \frac{1}{\hat{\theta}_2 x_4}[\frac{a_5}{c_3}|s_1|^\beta sgn(\frac{s_1}{\phi_1}) + \frac{a_6}{c_3}\int sgn(\frac{s_1}{\phi_1})dt \\ &\qquad -\hat{\theta}_2 x_3 + \hat{\theta}_1 x_3 - \dot{x}_{3ref}] \end{aligned}\right\} \tag{4.34}$$

Substituting the value of $\dot{\hat{\theta}}_1$, $\dot{\hat{\theta}}_2$, and $\dot{\hat{\theta}}_3$, and u_1, u_{23} and u_{45} from eq. (4.32) and eq. (4.34) respectively into eq. (4.31), It can be seen that $\dot{V} \leq 0$ which means the system meets the asymptotic stability property.

Table 4.3: PHEV simulation parameters

DC converters parameters	
Switching Frequency	$100kHz$
Inductance L_1, L_2, L_3	$100mH$
Resistance R_1, R_2, R_3	$20m\Omega$
Capacitance C_0	$15mF$
Gain parameters values	
Proposed nonlinear controller	Variables and values
AST-SMC controller	$c_1 = 0.01$ $c_2 = 0.1$ $c_3 = 0.1$ $c_4 = 0.1$ $a_1 = 1000$ $a_2, a_4, a_6 = 10$ $a_3, a_5 = 100$ $\phi_1, \phi_2, \phi_3, \phi_4 = 0.8$ $\alpha, \beta, \gamma = 0.6$

Chapter 5

Results and Discussions

In this section, the simulation results of the proposed AST-SMC controller for HESS of FC, supercapacitor and battery based PHEV are presented. The proposed controller is also compared with state of the art controllers. Simulation results of the proposed G2V charger are also presented using MATLAB/Simulink software. Finally, the simulation results are validated by comparing them with HIL results.

5.0.1 MATLAB simulation results

Tables 4.1, 4.2 and 4.3 show the model parameters used for performing simulations. Table 4.1 details the specifications of the G2V charger. Table 4.2 presents the parametric values of the HESS. Table 4.3 shows the nonlinear control design parameters followed by the values of adaptive gains for the proposed control system. The simulation results are presented in figs.. (5.1)-(5.9).

The proposed AST-SMC controller is tested using extra urban driving cycle (EUDC) load profile [11] in which load current varies with varying speed and loads of EUDC. Load current variations are between –80A and 40A as shown in fig. (5.1). Figs. (5.2)-(5.4) show the current tracking for FC, supercapacitor and battery respectively. As FC has low power density, it is used for constant and low load conditions. During high load requirements, all three sources are used to keep up with the increasing demands of the PHEV. During load transients, supercapacitor is used to rapidly provide the required energy for a short duration. These figures show that the proposed AST-SMC controller successfully tracks all the reference currents. Fig. (5.5) shows that the proposed controller tracks the desired DC bus voltage (400 Volts). Fig. (5.6) shows that the proposed AST-SMC controller performs better than Lyapunov redesign, synergetic and SMC based controllers as they take some time to reach the desired voltage. The proposed controller settles to the desired value within negligible time but SMC has chattering problem. The proposed controller has zero steady state error but Lyapunov based controller has some steady state error. Figs. (5.7) and (5.8) show the error and input signals respectively. Fig. (5.9) shows that the proposed G2V charger performs well and keeps the battery voltage to the desired value of 24 volts. It is clear that the proposed charger has faster response and safer operation. Overshoot of the proposed charger can be further reduced by using filters and signal processing techniques.

5.0.2 AST-SMC controller hard in loop results:

For further verification of the proposed AST-SMC controller, the proposed scheme is implemented on real-time HIL controller. Fig. (5.10) shows the experimental setup consisting of MS320F2837xD dual-core delfino microcontroller, personal computer, and MATLAB/Simulink software.

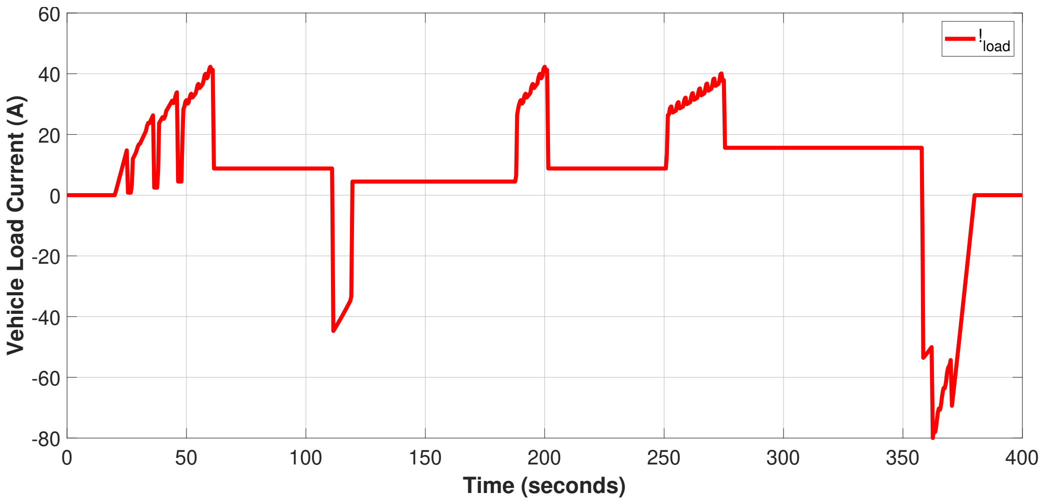

Figure 5.1: Varying load current profile for PHEV

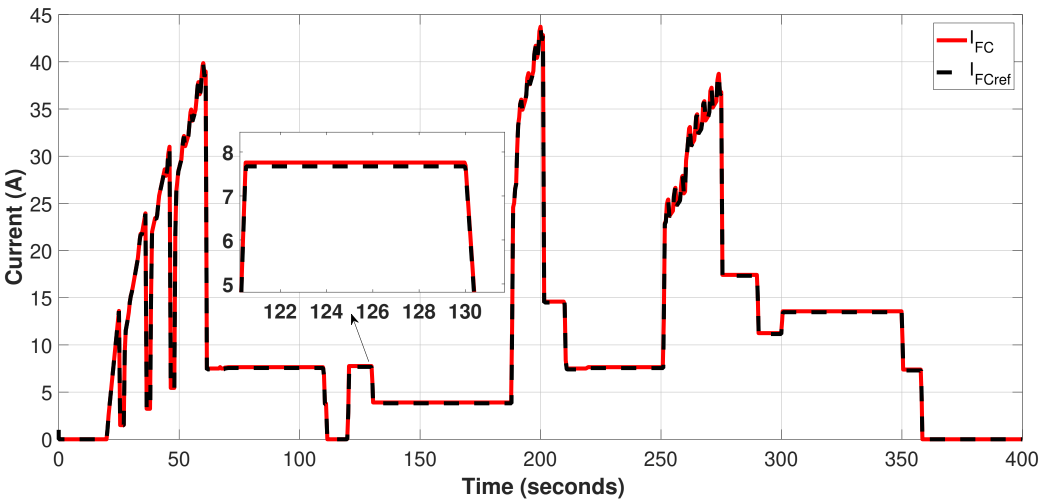

Figure 5.2: Fuel cell tracking current

The plant model of PHEV has been simulated in MATLAB/Simulink and then converted to executable code for performing the HIL. After this, the executed code is burnt into the dual-core delfino microcontroller for the generation of pulse width modulation for switching of the DC-DC converter. The plant has been simulated for 50s time to facilitate the EUDC speed profile of the vehicle. The matlab simulation results are then compared with HIL results to check the performance of the

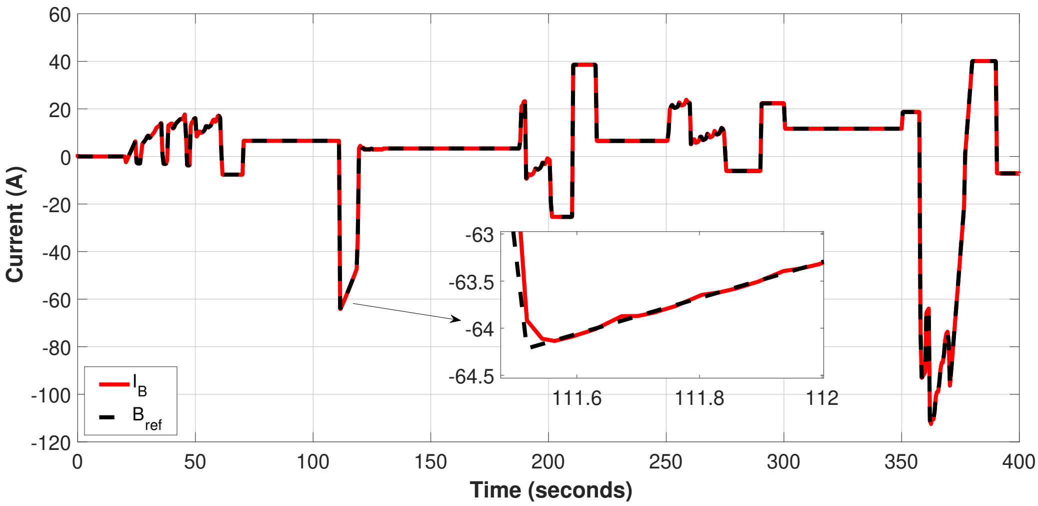

Figure 5.3: Battery tracking current

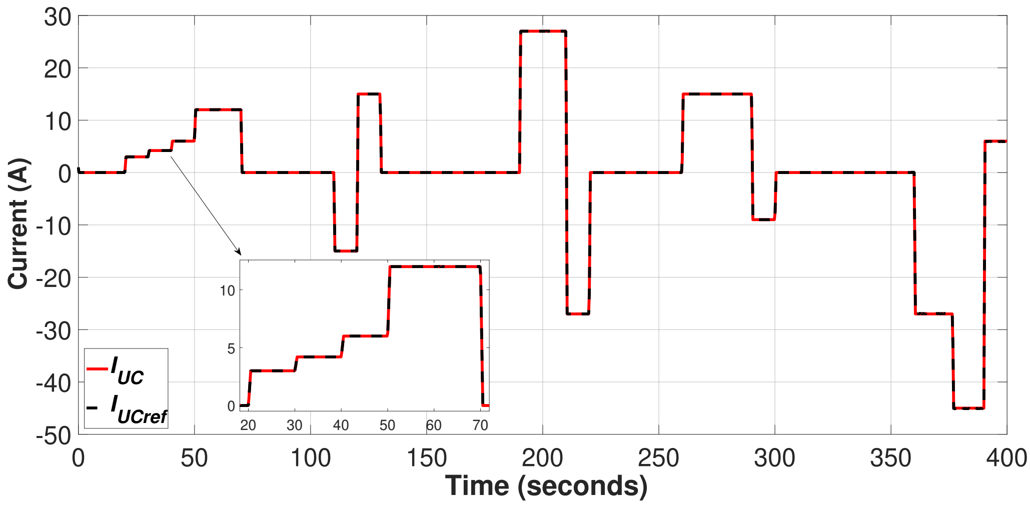

Figure 5.4: Supercapacitor tracking current

controller in real-time application.

Fig. (5.11) shows HIL results for DC bus voltage response. Few oscillations are observed in the figure, but the overall performance of the controller is up to the mark. It can be seen that the DC bus voltage is maintained and regulated at 400 volts.

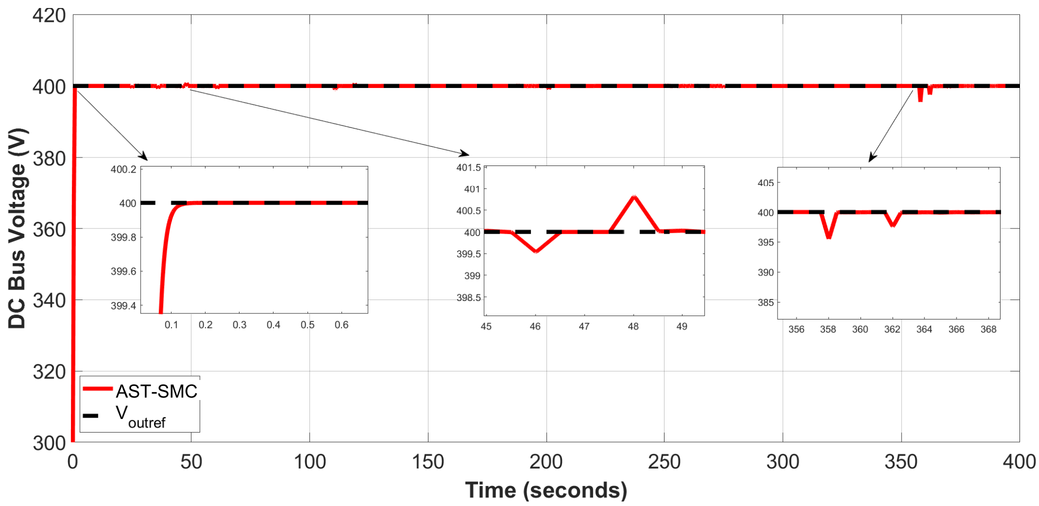

Figure 5.5: DC bus voltage

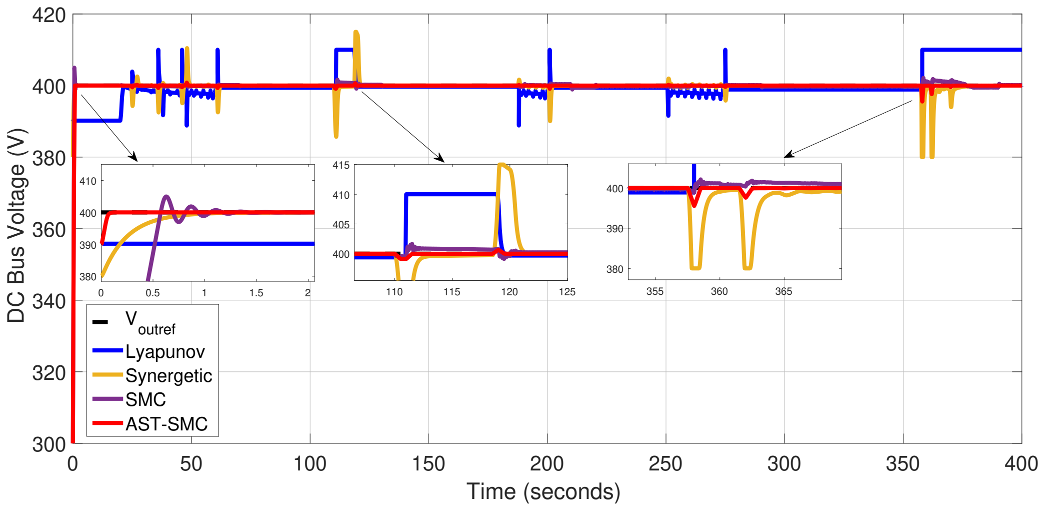

Figure 5.6: DC Bus voltage comparison.

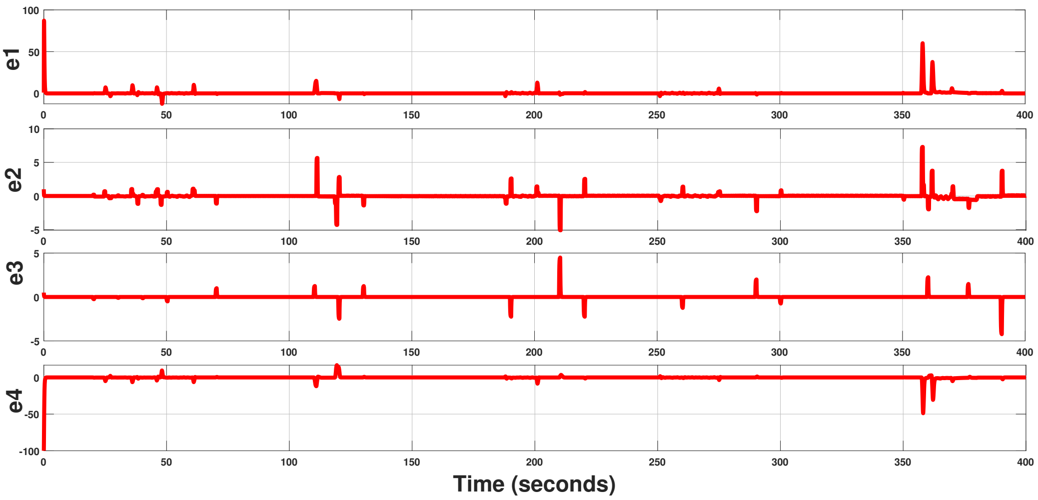

Figure 5.7: Power sources current tracking errors

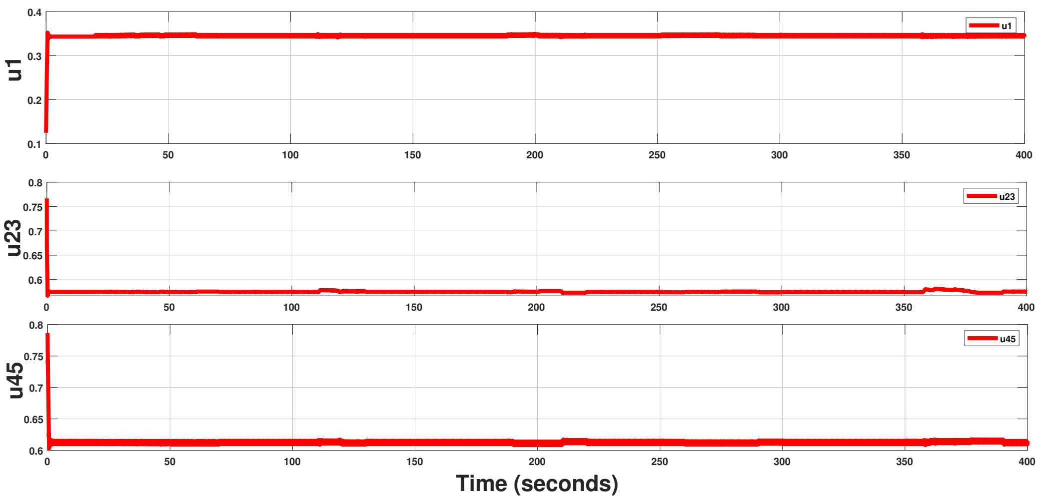

Figure 5.8: Control inputs signals

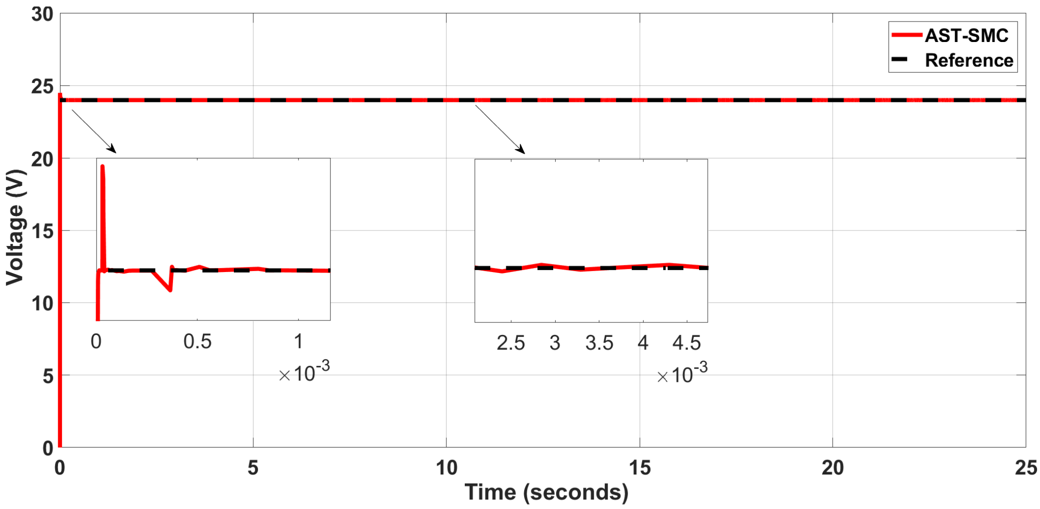

Figure 5.9: Charging voltage of G2V charger of PHEV

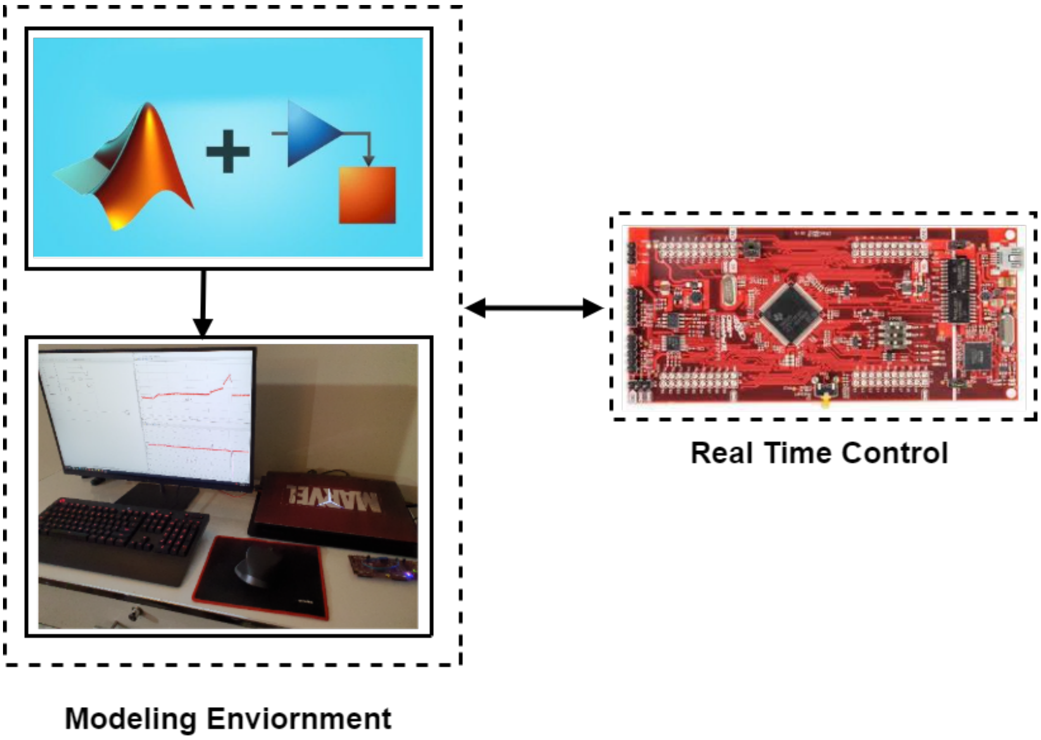

Figure 5.10: HIL setup used for hardware verification

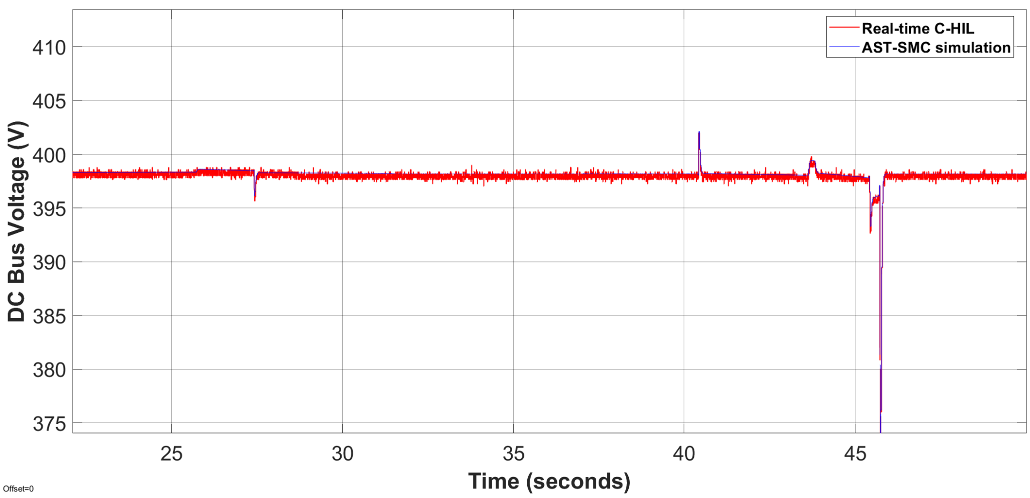

Figure 5.11: HIL DC bus voltage

Chapter 6

Conclusion and Future Work

6.1 Conclusion

In this research, AST-SMC is proposed for the regulation of DC bus voltage of the FC, battery and supercapacitor based PHEV. FC is the primary power source whereas battery and supercapacitor are the auxiliary sources. A G2V charger is proposed for faster and safer charging of PHEV. AST-SMC is used to regulate G2V charger voltage, DC bus voltage of HESS, and to maintain the power balance among the sources. Lyapunov stability analysis shows that the proposed system is asymptotically stable in the presence of load variations and parametric uncertainties. Proposed controller is compared with Lyapunov redesign, synergetic controller, and conventional sliding mode controller. Comparative analysis shows that proposed controller is more robust to parametric variations and model uncertainties. Real-time validation of the proposed controller, is performed using HIL simulation. Results show that the proposed controller regulates the DC bus voltage under all load conditions and has a good transient response.

6.2 Future Work

In future, the Hybrid energy storage system can be improved by adding more power sources. The energy management system could be refined using artificial intelligence (AI), artificial neural network (ANN) and advance nonlinear controller. To optimize parameters used in the energy management system can be optimized using different optimization algorithms. Size of the DC-DC converters can be reduced to reduce the size and cost of the over all system. Additionally, actual implementation of PHEV can be done in laboratory.

Bibliography

[1] D. Xu, Q. Liu, W. Yan, and W. Yang, "Adaptive terminal sliding mode control for hybrid energy storage systems of fuel cell, battery and supercapacitor," *Ieee Access*, vol. 7, pp. 29 295–29 303, 2019.

[2] A. U. Rahman, I. Ahmad, and A. S. Malik, "Variable structure-based control of fuel cell-supercapacitor-battery based hybrid electric vehicle," *Journal of Energy Storage*, vol. 29, p. 101365, 2020.

[3] K. Jiao and X. Li, "Water transport in polymer electrolyte membrane fuel cells," *Progress in energy and combustion Science*, vol. 37, no. 3, pp. 221–291, 2011.

[4] Y.-X. Wang, K. Ou, and Y.-B. Kim, "Modeling and experimental validation of hybrid proton exchange membrane fuel cell/battery system for power management control," *International Journal of Hydrogen Energy*, vol. 40, no. 35, pp. 11 713–11 721, 2015.

[5] H. Jiang, L. Xu, J. Li, Z. Hu, and M. Ouyang, "Energy management and component sizing for a fuel cell/battery/supercapacitor hybrid powertrain based on two-dimensional optimization algorithms," *Energy*, vol. 177, pp. 386–396, 2019.

[6] Y.-X. Wang, K. Ou, and Y.-B. Kim, “Power source protection method for hybrid polymer electrolyte membrane fuel cell/lithium-ion battery system,” *Renewable Energy*, vol. 111, pp. 381–391, 2017.

[7] H. He, S. Quan, and Y.-X. Wang, “Hydrogen circulation system model predictive control for polymer electrolyte membrane fuel cell-based electric vehicle application,” *International Journal of Hydrogen Energy*, vol. 45, no. 39, pp. 20 382–20 390, 2020.

[8] D.-J. Xuan, Z. Shi, J. Chen, C. Zhang, and Y.-X. Wang, “Real-time estimation of state-of-charge in lithium-ion batteries using improved central difference transform method,” *Journal of Cleaner Production*, vol. 252, p. 119787, 2020.

[9] L. Zhang, X. Hu, Z. Wang, F. Sun, J. Deng, and D. G. Dorrell, “Multiobjective Optimal Sizing of Hybrid Energy Storage System for Electric Vehicles,” *IEEE Transactions on Vehicular Technology*, vol. 67, pp. 1027–1035, 2018.

[10] J. Chen and Q. Song, “A decentralized dynamic load power allocation strategy for fuel cell/supercapacitor-based apu of large more electric vehicles,” *IEEE Transactions on Industrial Electronics*, vol. 66, no. 2, pp. 865–875, 2018.

[11] H. Armghan, I. Ahmad, N. Ali, M. F. Munir, S. Khan, and A. Armghan, “Nonlinear Controller Analysis of Fuel Cell,Battery, Ultracapacitor-based Hybrid Energy Storage Systems in Electric Vehicles,” *Arabian Journal for Science and Engineering*, vol. 43, pp. 3123–3133, 2018.

[12] H. Armghan, M. Yang, M. Q. Wang, N. Ali, and A. Armghan, “Nonlinear integral backstepping based control of a DC microgrid with renewable generation and energy storage systems,” *International Journal of Electrical Power and Energy Systems*, vol. 117, 2020.

[13] A. Rachid, H. E. Fadil, F. Belhaj, K. Gaouzi, and F. Giri, “Lyapunov-based control of single-phase ac–dc power converter for bev charger,” in *Recent Advances in Electrical and Information Technologies for Sustainable Development*. Springer, 2019, pp. 115–121.

[14] H. Armghan, I. Ahmad, N. Ali, M. F. Munir, S. Khan, and A. Armghan, “Nonlinear controller analysis of fuel cell–battery–ultracapacitor-based hybrid energy storage systems in electric vehicles,” *Arabian Journal for Science and Engineering*, vol. 43, no. 6, pp. 3123–3133, 2018.

[15] M. S. Nazir, I. Ahmad, M. J. Khan, Y. Ayaz, and H. Armghan, “Adaptive control of fuel cell and supercapacitor based hybrid electric vehicles,” *Energies*, vol. 13, no. 21, p. 5587, 2020.

[16] M. K. Azeem, H. Armghan, I. Ahmad, M. Hassan *et al.*, “Multistage adaptive nonlinear control of battery-ultracapacitor based plugin hybrid electric vehicles,” *Journal of Energy Storage*, vol. 32, p. 101813, 2020.

[17] S. S. Zehra, A. U. Rahman, H. Armghan, I. Ahmad, and U. Ammara, “Artificial intelligence-based nonlinear control of renewable energies and storage system in a dc microgrid,” *ISA transactions*, 2021.

[18] W. Redman-White, H. Kennedy, R. Bodnar, and T. Lee, “Adaptive tuning of large-signal resonant circuits using phase-switched fractional capacitance,”

IEEE Transactions on Circuits and Systems II: Express Briefs, vol. 64, no. 9, pp. 1072–1076, 2016.

[19] M. Hannan, F. Azidin, and A. Mohamed, "Hybrid electric vehicles and their challenges: A review," *Renewable and Sustainable Energy Reviews*, vol. 29, pp. 135–150, 2014.

[20] F. Zhang, X. Zhang, M. Zhang, and A. S. Edmonds, "Literature review of electric vehicle technology and its applications," in *2016 5th International Conference on Computer Science and Network Technology (ICCSNT)*. IEEE, 2016, pp. 832–837.

[21] J. Shangguan, H. Guo, and M. Yue, "Robust energy management of plug-in hybrid electric bus considering the uncertainties of driving cycles and vehicle mass," *Energy*, vol. 203, p. 117836, 2020.

[22] M. Olivares and P. Albertos, "Linear control of the flywheel inverted pendulum," *ISA transactions*, vol. 53, no. 5, pp. 1396–1403, 2014.

[23] A. Muntaser, H. Elwarfalli, A. Suleiman, and G. Subramanyam, "Design and implementation of conventional (pid) and modern (fuzzy logic) controllers for an energy storage system of hybrid electric vehicles," in *2017 IEEE National Aerospace and Electronics Conference (NAECON)*. IEEE, 2017, pp. 267–270.

[24] A. Tahri, H. El Fadil, F. Giri, and F. Z. Chaoui, "A lyapunov based power management for a fuel cell hybrid power source for electric vehicle," in *2015 3rd International Renewable and Sustainable Energy Conference (IRSEC)*. IEEE, 2015, pp. 1–6.

[25] R. Dhaouadi, K. Khosravi, and Y. Hori, "Synergetic control of a hybrid battery-ultracapacitor energy storage system," in *Advancements in Energy Storage Technologies*. IntechOpen, 2018.

[26] M. F. Munir, I. Ahmad, S. A. Siffat, M. A. Qureshi, H. Armghan, and N. Ali, "Non-linear control for electric power stage of fuel cell vehicles," *ISA transactions*, vol. 102, pp. 117–134, 2020.

[27] A. Boonyaprapasorn, P. S. Ngiamsunthorn, and T. Sethaput, "Synergetic control for hiv infection system of cd4+ t cells," in *2016 16th International Conference on Control, Automation and Systems (ICCAS)*. IEEE, 2016, pp. 484–488.

[28] H. Armghan, M. Yang, M. Wang, N. Ali, and A. Armghan, "Nonlinear integral backstepping based control of a dc microgrid with renewable generation and energy storage systems," *International Journal of Electrical Power & Energy Systems*, vol. 117, p. 105613, 2020.

[29] H. El Fadil and F. Giri, "Sliding mode control of fuel cell and supercapacitor hybrid energy storage system," *IFAC Proceedings Volumes*, vol. 45, no. 21, pp. 669–674, 2012.

[30] M. Yilmaz and P. T. Krein, "Review of battery charger topologies, charging power levels, and infrastructure for plug-in electric and hybrid vehicles," *IEEE Transactions on Power Electronics*, vol. 28, pp. 2151–2169, 2013.

[31] C. Xia and C. Zhang, "Power management strategy of hybrid electric vehicles based on quadratic performance index," *Energies*, vol. 8, pp. 12 458–12 473, 2015.

[32] S. Kumar and A. Usman, "A review of converter topologies for battery charging applications in plug-in hybrid electric vehicles," *IEEE Industry Applications Society Annual Meeting, IAS*, pp. 1–9, 2018.

[33] S. East and M. Cannon, "Energy Management in Plug-In Hybrid Electric Vehicles: Convex Optimization Algorithms for Model Predictive Control," vol. 28, pp. 2191–2203, 2020.

[34] J. R. Szymanski, M. Zurek-Mortka, D. Wojciechowski, and N. Poliakov, "Unidirectional DC/DC converter with voltage inverter for fast charging of electric vehicle batteries," *Energies*, vol. 13, pp. 1–17, 2020.

[35] J. H. Lee, D. Y. Jung, S. H. Park, T. K. Lee, Y. R. Kim, and C. Y. Won, "Battery charging system for PHEV and EV using single phase AC/DC PWM buck converter," *Journal of Electrical Engineering and Technology*, vol. 7, pp. 736–744, 2012.

[36] B. Singh, B. N. Singh, A. Chandra, K. Al-Haddad, A. Pandey, and D. P. Kothari, "A review of single-phase improved power quality AC-DC converters," *IEEE Transactions on Industrial Electronics*, vol. 50, pp. 962–981, 2003.

[37] S. Lacroix, S. Member, E. Laboure, and M. Hilairet, "An Integrated Fast Battery Charger for Electric Vehicle," *IEEE Vehicle Power and Propulsion Conference*, 2010.

[38] M. Tali, A. Obbadi, A. Elfajri, and Y. Errami, "Passive filter for harmonics mitigation in standalone PV system for non linear load," *Proceedings of 2014*

International Renewable and Sustainable Energy Conference, IRSEC 2014, pp. 499–504, 2014.

[39] A. M. Haidar and K. M. Muttaqi, "Behavioral characterization of electric vehicle charging loads in a distribution power grid through modeling of battery chargers," *IEEE Transactions on Industry Applications*, vol. 52, pp. 483–492, 2016.

[40] B. Jiang, D. Xu, P. Shi, and C. C. Lim, "Adaptive neural observer-based backstepping fault tolerant control for near space vehicle under control effector damage," *IET Control Theory & Applications*, vol. 8, no. 9, pp. 658–666, 2014.

[41] W. Sun, Y. Zhang, Y. Huang, H. Gao, and O. Kaynak, "Transient-performance-guaranteed robust adaptive control and its application to precision motion control systems," *IEEE Transactions on Industrial Electronics*, vol. 63, no. 10, pp. 6510–6518, 2016.

[42] M. S. Khan, I. Ahmad, and F. Z. U. Abideen, "Output voltage regulation of fc-uc based hybrid electric vehicle using integral backstepping control," *IEEE Access*, vol. 7, pp. 65 693–65 702, 2019.